

# Synthesis of Boron Nitride Coating on Carbon Nanotubes

Linlin Chen, Haihui Ye, and Yury Gogotsi\*

Department of Materials Science and Engineering, Drexel University, Philadelphia, Pennsylvania 19104

**A method to synthesize boron nitride coating on the surface of carbon nanotubes (nanofibers) without damaging the tube walls has been developed. A reaction between boric acid and ammonia was performed at moderate temperatures on the surface of carbon nanotubes to form boron nitride (BN) coatings. The surface structure of the carbon nanotubes significantly influences the morphology of the boron nitride coating. If the surface of the tubes is free of defects, highly crystallized insulating BN nanotubes can encapsulate carbon nanotubes. On the surface of carbon nanotubes with disordered wall structure, a polycrystalline BN sheath was produced.**

## I. Introduction

DISCOVERY of carbon nanotubes (CNTs)<sup>1</sup> has attracted significant interest to nanoscale one-dimensional structures and led to the development of a number of novel 1-D materials including ceramic nanotubes, nanofibers, and nanorods.<sup>2,3</sup> Their diameter is at least an order of magnitude smaller than that of the long and short fibers or whiskers that are currently used. Boron nitride (BN) nanotubes in particular have received much attention<sup>4,5</sup> because they are insulating, do not react with molten metals, and have higher oxidation resistance than carbon. Thus, they have many useful properties that carbon nanotubes do not have. Nanotubes containing separated BN and carbon layers have been synthesized by arc discharge.<sup>6</sup> Heterogeneous growth of B–C–N nanotubes has also been achieved by laser ablation.<sup>7</sup> Both of these methods, however, have low yields and high cost. Therefore, there is still no commercial production of BN nanotubes or nanofibers. The common synthesis methods require introduction of Fe, Ni, or Na,<sup>2–4</sup> which contaminates the final product and limits applications of the BN nanotubes. Purification of BN is more difficult than that of CNT, because BN reacts with water and therefore wet chemical methods cannot be used. On the other hand, multiwall carbon nanotubes are produced by many companies at a reasonable cost, and their purification techniques have been well-developed. In particular, larger (50–200 nm in diameter) tubes which are often called carbon nanofibers are produced in large volumes that allow for a variety of applications. Therefore, using these tubes as templates or substrates to synthesize BN nanotubes is attractive.

B–C–N nanotubes have been produced by reacting carbon nanotubes with B<sub>2</sub>O<sub>3</sub> vapor and nitrogen at high temperatures (1300°–1700°C).<sup>8–10</sup> The crystallization of BN was found to preferentially take place at the inner and outer surface of the carbon nanotubes.<sup>9</sup> Combining the advantages of two materials

(e.g., BN coating on CNTs) would also be of great value for the design of nanoscale electronic devices and nanostructured composites. However, the production of BN layers by this method always leads to the consumption and destruction of carbon layers, which may result in the loss of the structural integrity of the tubes. In addition, the method requires relatively high temperatures and produces very thin layers of BN even at around 1500°C, which make it not economically viable. In the present work, we report a new coating method involving a reaction between boric acid and ammonia on the surface of carbon nanotubes at temperatures of 1100°–1200°C.

## II. Experimental Procedure

Two kinds of large Pyrograph<sup>®</sup> commercial carbon nanotubes (nanofibers) were used as starting materials: pyrolytically stripped carbon nanotubes (PS-CNTs) and heat-treated carbon nanotubes (HT-CNTs) annealed at 3000°C (Applied Sciences, Inc.). The tube walls of PS-CNTs and HT-CNTs before coating treatment are shown in Figs. 1(a) and (b), respectively. The average diameter (~100 nm) and wall thickness (15–20 nm) are similar for both grades, whereas the structure of the tube walls is apparently different. The outer graphite sheets of PS-CNTs (Fig. 1(a)) are partly disordered due to the thermal etching during the postproduction processing, leaving the surface of PS-CNTs disordered and turbostratic (Fig. 1(a)). For HT-CNTs, which have been heat-treated at 3000°C for a sufficiently long time, energetically and chemically stable arched edges<sup>11</sup> were formed as shown by arrows in Fig. 1(b). The “herringbone” structure of CNTs can be clearly seen in Fig. 1(b). Knowing the structure difference of the initial CNTs is crucial to understanding the BN growth on the CNTs.

The nanotubes were characterized by using environmental scanning electron microscopy (ESEM: FEI XL-30), energy-dispersive X-ray spectroscopy (EDS), high-resolution transmission electron microscopy (HRTEM), and electron energy loss spectroscopy (EELS) measurements. The TEM images and EELS spectra were acquired by using a field emission TEM (JEOL-2010F) with an accelerating voltage of 200 kV, equipped with a Gatan parallel EELS spectrometer. The line-scan EELS experiments were performed by scanning a finely focused electron probe across the nanotubes and recording the EELS spectra. The K edge intensities of C, B, and N were normalized to obtain concentration profiles.

A two-step process, including boric acid infiltration and subsequent nitridation, has been used. It is similar to the process we used to produce a BN coating on SiC fibers.<sup>12</sup> Boric acid was used as the most economical precursor for the synthesis of BN. Unlike metal borates used elsewhere, it does not contaminate the samples by metal impurities. A vacuum chamber was used to infiltrate saturated H<sub>3</sub>BO<sub>3</sub> solution into the CNT powders at 100°C.

After drying in air, infiltrated CNT powders were loaded in a quartz boat and placed into a horizontal quartz tube furnace. Before each experimental run, the furnace was purged with argon for at least 30 min. Then the furnace was heated to the desired operating temperature at a rate of 10°C/min with

M. Chowalla—contributing editor

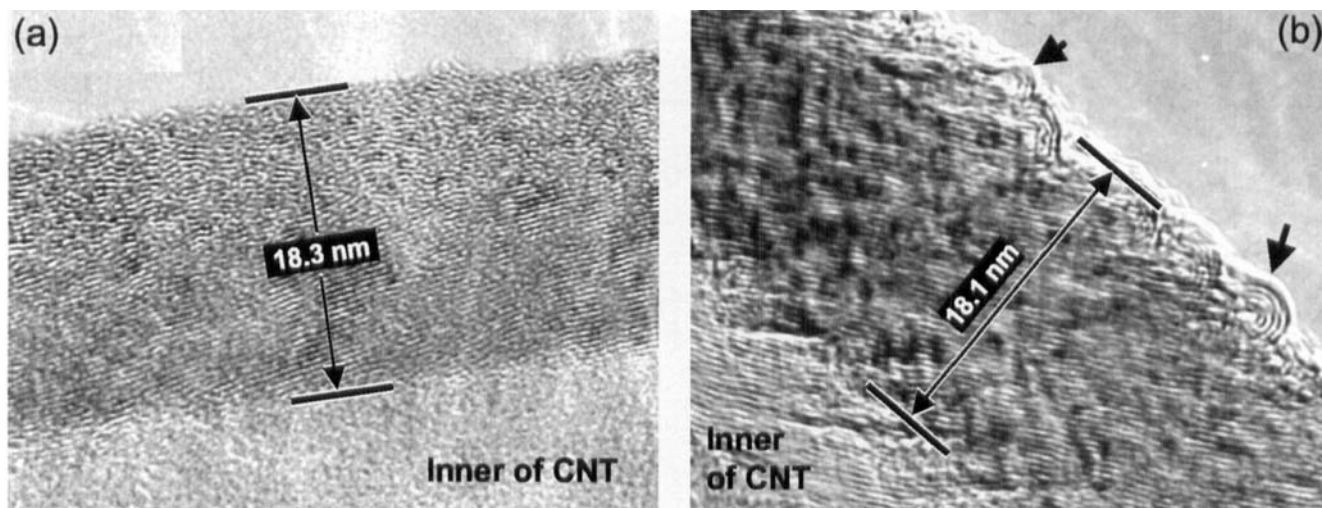


Fig. 1. HRTEM images of the tube walls of the PS-CNTs (a) and HT-CNTs (b) before coating. The arrows in (b) mark the arched graphite structure.

ammonia (grade 4, purity 99.99%, BOC gases) flowing into the reaction tube at a flow rate of 20 sccm. The sample was held at 1100°–1200°C for a desired period of time to secure the completion of the reaction and then cooled down in the furnace under the ammonia flow for protection. The thickness of the BN layers depends on the nitridation time—the longer the time, the thicker the BN coating formed—but nitridation kinetics will not be analyzed in this paper. The results are illustrated with the data obtained on the samples treated in ammonia at 1165°C for 50 min.

### III. Results and Discussion

The SEM study of the coated nanotubes shows that both tubes changed their appearance (Fig. 2). The bright appearance of the tubes in the SEM images shows that their conductivity was low and they were charging, unlike carbon nanotubes, which have high electrical conductivity. EDS analysis has shown the presence of boron and nitrogen along with carbon (Fig. 2(c)), confirming the formation of BN. It is also important to note that the HT-CNT was uniform and cylindrical (Fig. 2(b)), while the surface of PS-CNT looked rough (Fig. 2(a)).

TEM analysis confirms that the coating of PS-CNT is rough (Fig. 3(a)). The interface between the coating and the CNT is not clearly defined. The HRTEM image in Fig. 3(b) reveals that the coating consists of polycrystalline (columnar) BN. The lattice fringes in every individual BN crystal are highly ordered, but the orientation of the crystals is slightly different, which prohibits the joining of the crystals to form a single-crystalline coating. The lattice parameter of the crystals is  $\sim 0.33$  nm, which is consistent with the (002) spacing of 0.33 nm in bulk hexagonal BN. Basal planes of BN particles are oriented parallel to the tube axis. Some amount of amorphous phase is present at the grain boundaries. The thickness of the carbon wall under the BN coating is 18.5 nm, similar to the average thickness of the tube walls before coating (Fig. 1(a)). This suggests the growth of BN on the CNTs without any or with only minor consumption of the wall. The carbon remains disordered in the outer layers and well-aligned in the inner layers, indicating that the coating process does not change the structure of the CNTs.

A uniform crystalline coating is formed on the surface of HT-CNTs (Figs. 3(c,d)). Figure 3(c) shows that the coating is smooth, homogenous, and symmetric. Highly ordered lattice fringes of the coating can be seen in Fig. 3(d). The fact that the lattice spacing is 0.33 nm and exactly the same number of layers can be found on the other side of the tube wall strongly suggests that the coating is a BN nanotube encapsulating the carbon tube.

Therefore, a sort of new composite nanotube—a carbon nanotube covered by a BN nanotube—has been fabricated. The characteristic chirality of the carbon tube wall in HT-CNTs is maintained after coating treatment (compare Fig. 1(b) and Fig. 3(d)). The thickness of the carbon wall is about the same as the average thickness of the tube wall in HT-CNTs. Although most of the arched edges are invisible at the boundary between the carbon and BN layers, some can still be found, as indicated by arrows in Fig. 3(d). Since the arched structure is only present on the outermost surface of the HT-CNTs, partial disappearance of the characteristic structure simultaneously has two meanings: (1) several layers of carbon tube wall might have been removed during coating; (2) the thickness of the removed layers is limited in  $\sim 1$  nm (otherwise no arched edge should be found). It is important to note that the BN sheath has a cylindrical structure with layers parallel to the tube axis, unlike the herringbone structure of the core tube.

Line-scan EELS analyses of the BN-coated PS-CNTs and HT-CNTs along the lines indicated in Figs. 3(a) and (c) produced similar results, as shown in Fig. 4(a). It can be seen that the BN-rich phase is located at the outer tube surface while the carbon-rich phase is inside, which is in agreement with the HRTEM results. Three representative EELS spectra, obtained by moving the electron probe from the inner tube wall to the edge of the coating, are compared in Fig. 4(b). Two intense peaks, one starting at 188 eV and another at 401 eV, correspond to the B-K and N-K edges, respectively. The quantified B/N ratio is close to 1.0, namely, the stoichiometric composition of BN. No carbon signal (C-K edge, at 284 eV) is visible in the spectrum from the tube edge of HT-CNTs, whereas a small amount of carbon can be detected sometimes in the coating of PS-CNTs, probably due to the presence of amorphous B-C-N phase between the BN crystals (Fig. 3(b)). The sharp profiles of  $\pi^*$  peaks for both B-K and N-K edges confirm the  $sp^2$ -type bonding. The increase of the ratio between the  $\pi^*$  and  $\sigma^*$  peaks for the B-K edge from the center to the edge is the result of changing orientation of the electron beam with respect to the BN layers.<sup>6</sup> It is not surprising to observe such evolution in the BN tubular coating on HT-CNTs. Similar observation in BN-coated PS-CNTs indicates that the BN nanocrystals are aligned roughly parallel to the CNT axis, such as tile covering the tube.

Both HRTEM and EELS do not show the presence of BN inside the CNTs. Gray spots inside the nanotube in Fig. 3(a) are due to the projection of BN crystals on the front and back surfaces of the CNT. Apparently, the boric acid did not penetrate into the CNTs or ammonia access to the inside of the tube was not sufficient to initiate the reaction.

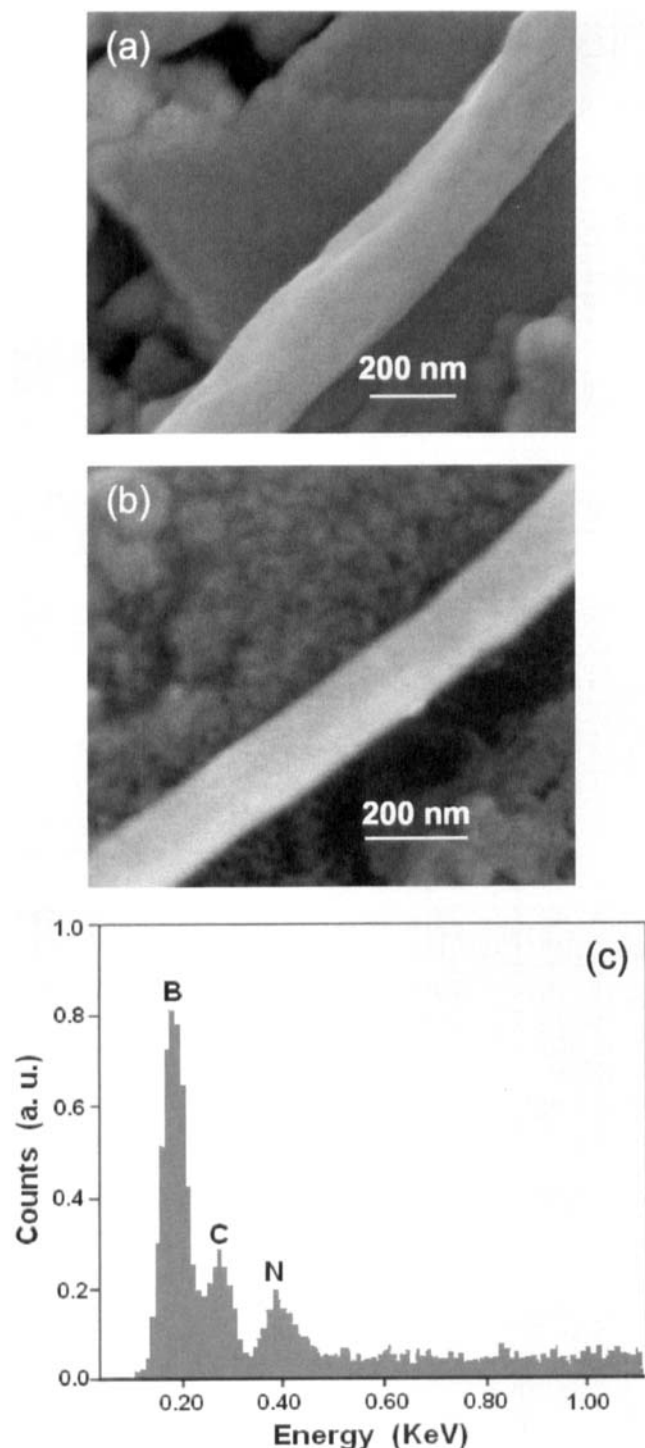
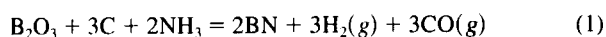


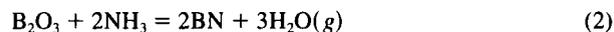
**Fig. 2.** SEM images of PS-CNT (a) and HT-CNT (b) after coating and EDS spectrum of the BN-coated HT-CNT (c).

The initial reaction of BN formation may start between boron oxide (dehydrated from boric acid at elevated temperature), carbon (from the surface of CNTs), and ammonia according to the thermodynamic calculation:<sup>12</sup>



This reaction accounts for the removal of the surface layer of the CNTs and nucleation of BN (Fig. 3(d)). The BN produced may form the seed layers on the surface of the CNTs. Due to the relatively low synthesis temperature, the newly formed BN layer acts as a diffusion barrier, preventing further reaction of

$\text{B}_2\text{O}_3$  with carbon. Then boron oxide directly reacts with ammonia to form BN in the lack of carbon:



The thermodynamic probability of this reaction is low. However, the flow of ammonia gas, and that water vapor is removed instantly, may shift the reaction to the right. The result of the reaction is accumulation and growth of hexagonal BN crystals on the CNT surface.

Here, the different surface structure of two CNT grades plays an important role in the growth of BN. Because the surface of PS-CNTs is turbostratic (Fig. 1(a)), nucleation of BN crystals occurs easily in many places on the tube surface. However, BN seeds have different orientations and are not exactly parallel to the tube surface, thus forming a polycrystalline coating. Amorphous interlayers separate BN nanocrystals. Such polycrystalline structure is typical in the synthesis of BN coating on the bulk materials.<sup>13,14</sup> The nucleation of BN on the ordered and chemically stable surfaces of HT-CNT by reaction (1) is difficult at this low temperature. Once a single BN nucleus forms on the surface of a CNT, further growth of BN by reaction (2) would occur by adding boron and nitrogen atoms to the edge of the nucleus, enabling the growth of a single layer of BN. Eventually, a new layer appears on the surface of BN and several layers can grow depending on the synthesis time and amount of boron available. This leads to synthesis of a single crystalline BN nanotube as a sheath on the surface of the CNT. Although HT-CNT has a herringbone wall structure, it has a cylinder-like surface, when seen at a smaller magnification. The growing BN nanotube will follow the shape of the carbon tube, because van der Waals forces will keep the BN sheet attached to the graphite substrate, while the elastic forces in the planar structure of BN will not allow the growing sheet to follow the surface topology exactly and will result in the cylindrical overgrowth. The mismatch between the cylindrical BN wall and the herringbone carbon wall can be seen in Fig. 3(d) as white triangular spacing. It may be filled with amorphous carbon and/or BN.

Although this study was conducted on large-diameter multiwall nanotubes (nanofibers), it is obvious that the same process can be used to produce BN coatings on much smaller nanotubes or much larger carbon fibers. However, as this work has shown, the surface structure of carbon affects the structure of the BN coating.

Such composite nanotubes could have application as reinforcement in ceramic and metal matrix composites. For example, they can be used to reinforce carbide-forming metals, which would react with carbon. They can also be used in high-temperature composites, providing a much higher oxidation resistance compared with carbon, or in insulating electronic substrates, where high thermal conductivity of carbon nanotubes needs to be combined with the high electrical resistivity of BN. Nanotube C-BN heterostructures may have attractive electronic properties. The BN-coated carbon nanotubes can be used as insulated nanowires in nanoelectronics. Insulating coatings on carbon nanotubes may also allow electrophoretic transport of liquid through the tube channel.

#### IV. Conclusions

A process for synthesis of BN coating on the surfaces of carbon nanotubes and nanofibers has been developed. The coatings are produced by a simple and inexpensive method from boric acid and ammonia around 1150°C. The two-step process includes infiltration of nanotubes with boric acid and nitridation in ammonia. After epitaxial BN nucleation on the CNT surface, boron oxide reacts directly with ammonia without further consumption of the CNTs. The tube wall structure of the CNTs controls the nucleation and structure of BN coatings. Disordered turbostratic surfaces lead to the polycrystalline BN coating, while a defect-free surface results in the highly crystallized BN nanotube covering the CNT. BN

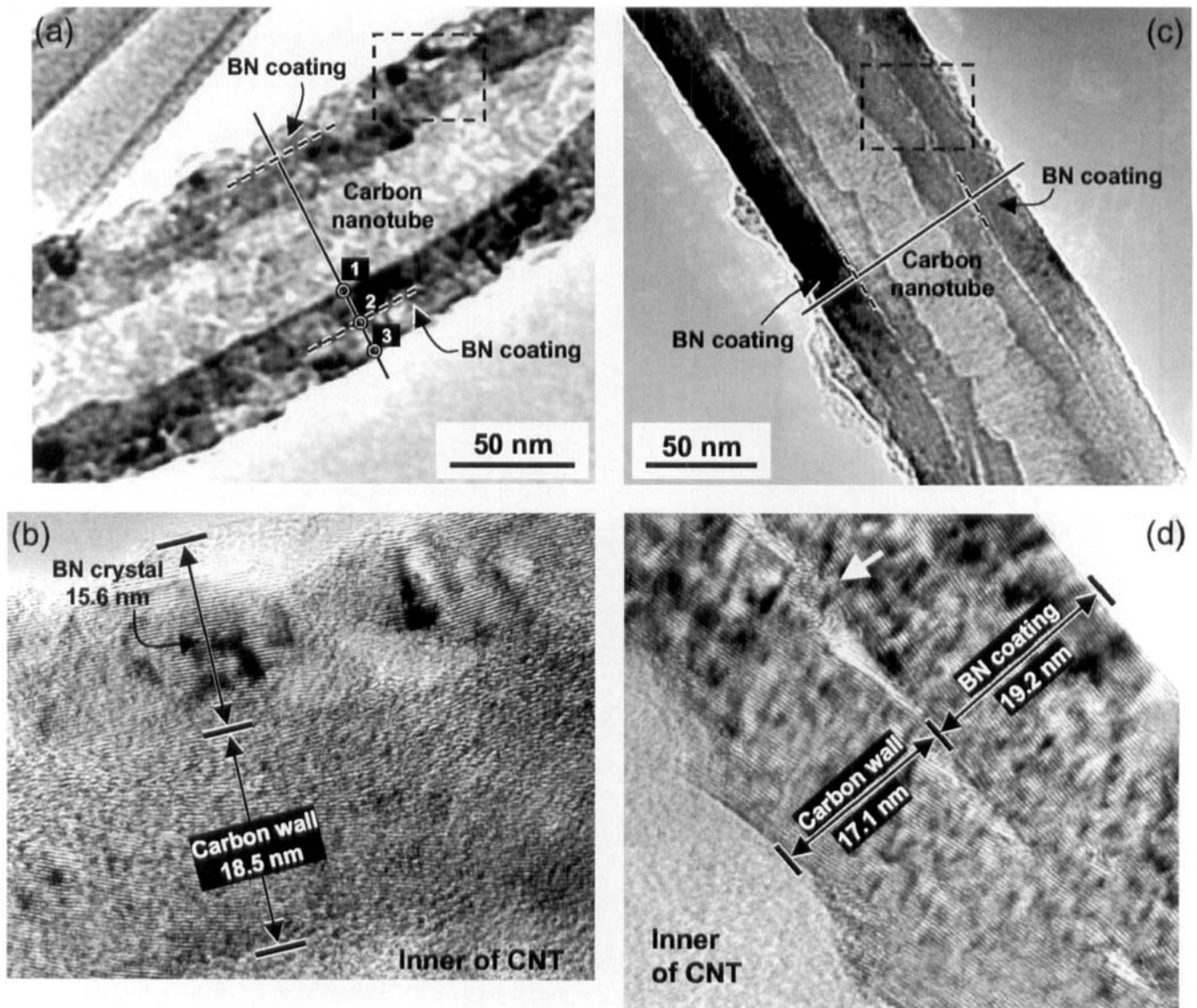


**Fig. 3.** TEM image of a BN-coated PS-CNTs (a,b) and HT-CNTs (c,d). The solid lines indicate the line-scan EELS analysis; (b) and (d) are HRTEM images of the framed regions in (a) and (c), respectively.

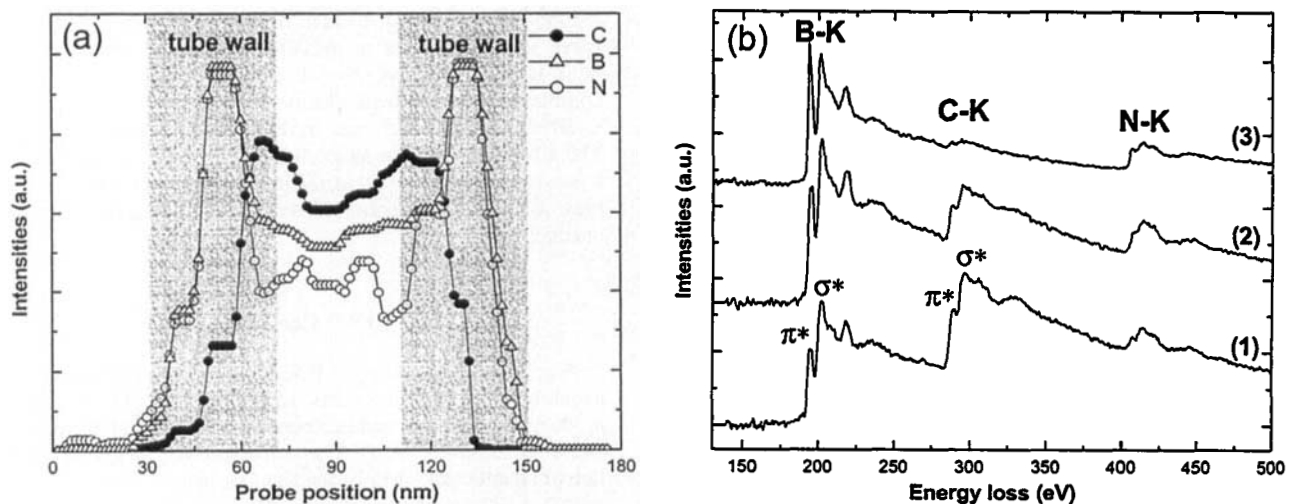


**Fig. 4.** EELS analysis of a BN-coated PS-CNT: (a) normalized concentration profiles of B, C, and N across the nanotube (along the line shown in Fig. 3(a)); the positions of the tube walls are shown by gray bands; (b) evolution of EELS spectra of the nanotube from the inner tube wall (spot 1 in Fig. 3(a)) to the edge of the BN coating (spot 3), demonstrating the near-edge fine structure of B, C, and N. Similar EELS analysis results have been obtained from the BN-coated HT-CNT along the line shown in Fig. 3(c).

coatings form on the surface of CNTs without damaging the carbon walls.

### Acknowledgments

We are thankful to Professor J.-C. Bradley (Drexel University) for providing nanotube samples. TEM work was done in LRSM, University of Pennsylvania.

### References

<sup>1</sup>S. Iijima, "Helical Microtubules of Graphitic Carbon," *Nature (London)*, **354**, 56–58 (1991).

<sup>2</sup>P. Harris, *Carbon Nanotubes and Related Structures*; pp. 16–54. Cambridge University Press, Cambridge, U.K., 1999.

<sup>3</sup>M. Terrones, N. Grobert, and H. Terrones, "Synthetic Routes to Nanoscale B<sub>x</sub>C<sub>y</sub>N<sub>z</sub> Architectures," *Carbon*, **40**, 1665–84 (2002).

<sup>4</sup>L. A. Chernozatonskii, E. G. Galpern, I. V. Stankevich, and Y. K. Shimkus, "Nanotube C–BN Heterostructures: Electronic Properties," *Carbon*, **37**, 117–21 (1999).

<sup>5</sup>D. Golberg, Y. Bando, M. Mitome, K. Kurashima, N. Grobert, M. Reyes-Reyes,

H. Terrones, and M. Terrones, "Nanocomposites: Synthesis and Elemental Mapping of Aligned B–C–N Nanotubes," *Chem. Phys. Lett.*, **360**, 1–7 (2002).

<sup>6</sup>K. Suenaga, C. Colliex, N. Demoncey, A. Loiseau, H. Pascard, and F. Willaime, "Synthesis of Nanoparticles and Nanotubes with Well-Separated Layers of Boron Nitride and Carbon," *Science (Washington, D.C.)*, **278**, 653–55 (1997).

<sup>7</sup>Y. Zhang, H. Gu, K. Suenaga, and S. Iijima, "Heterogeneous Growth of B–C–N Nanotubes by Laser Ablation," *Chem. Phys. Lett.*, **279**, 264–69 (1997).

<sup>8</sup>W. Han, Y. Bando, K. Kurashima, and T. Sato, "Synthesis of Boron Nitride Nanotubes from Carbon Nanotubes by a Substitution Reaction," *Appl. Phys. Lett.*, **73**, 3085–87 (1998).

<sup>9</sup>Y. Bando, D. Golberg, M. Mitome, K. Kurashima, and T. Sato, "C to BN Conversion in Multi-walled Nanotubes As Revealed by Energy-Filtering Transmission Electron Microscopy," *Chem. Phys. Lett.*, **346**, 29–34 (2001).

<sup>10</sup>D. Golberg, Y. Bando, K. Kurashima, and T. Sato, "Ropes of BN Multi-walled Nanotubes," *Solid State Commun.*, **116**, 1–6 (2000).

<sup>11</sup>S. V. Rotkin and Y. Gogotsi, "Analysis of Non-planar Graphitic Structures: From Arched Edge Planes of Graphite Crystals to Nanotubes," *Mater. Res. Innovations*, **5**, 191–200 (2002).

<sup>12</sup>L. Chen, H. Ye, Y. Gogotsi, and M. J. McNallan, "A Novel Method for Synthesis of BN Coatings on SiC," *J. Am. Ceram. Soc.*, **86** [11] 1830–37 (2003).

<sup>13</sup>P. B. Mirkarimi, K. F. McCarty, and D. L. Medlin, "Review of Advances in Cubic Boron Nitride Film Synthesis," *Mater. Sci. Eng.*, **21**, 47–100 (1997).

<sup>14</sup>S. P. S. Arya and A. D. Amico, "Preparation, Properties and Applications of Boron Nitride Thin Film," *Thin Solid Films*, **157**, 267–82 (1988). □